Underwater Pipelines

Team Members: Conor Brew, Steven Ma, Nadiah Zamri

Summary

Undersea oil and gas pipelines are critical to the world's energy infrastructure. The mechanical, thermal, and chemical environment they are subjected to demands high-performance materials to prevent failure.

Performance metrics

Loads: Pipelines in undersea environments are subjected to a variety of loads. These include hydrostatic pressure, water currents, and thermal gradients [1]. In addition, segments of the pipe suspended between parts of the seaflooor experience bending. They are often designed to last up to 50 years [1]. Proper design and material selection can help to account for these factors and ensure the structural integrity of the pipeline.

- *Hydrostatic pressure* The hydrostatic pressure underwater increases with the depth of the pipeline, and it can range from a few hundred PSI (pounds per square inch) for shallow pipelines to over 10,000 PSI for deep pipelines. [2]
- *Temperature gradients* Temperature gradients result from the temperature differences between pipelines and surrounding water, which can lead to thermal expansion and contraction of the pipeline. The oil temperature can be up to 100 degrees Celsius, and external temperatures as low as 5 degrees Celsius. [3]
- *Bending* The amount of bending force that a pipeline is subjected to can vary depending on several factors, such as the water current, the weight of the pipeline, and the changes in the seabed topography. The performance metrics for these conditions can be modelled using bending moments experienced by

the pipelines. This depends on the depth of the pipeline. For example, a pipeline located in a deepwater environment (more than 1000 meters water depth) with a design factor of 0.72 can withstand a maximum allowable bending moment of 110,000 Nm/m. [4]

Chemical corrosion: Underwater pipelines are subject to external corrosion due to CO_2 and H_2S in water. Therefore, to prevent corrosion, the external surface of underwater pipelines is commonly coated and further protected with cathodic protection systems or galvanization.

- *External coating* Typical commercial coatings for metal pipelines consist of polymer-based coatings, such as fusion epoxy bonded coating (FBE), polyolefin, neoprene, and polypropylene. Hence, the selection of pipeline material must be compatible with these coatings to ensure commercial viability.
- *Material composition* In regards to the composition of the material, chromium is often added to the metal alloy matrix to form a layer of chromium oxide when reacting with oxygen, which protects the material from corrosion. However, the significant volume of material required for underwater pipelines means that increasing the chromium composition can be prohibitively expensive. Therefore, optimizing the balance between cost and desired chemical properties is key as the overall cost is a design constraint.

Figure 1: Rig with pipes to be laid [5]

System Design Chart

The system design chart in Figure 2 presents the relevant processing, structure, properties, and performance parameters, as well as their connections. The primary goal of this materials design is to maximize performance pipe resistance to loads and corrosion while taking into account cost, design architecture, and manufacturability constraints.

Note: expand on key parameters (the 4, and add constraints)

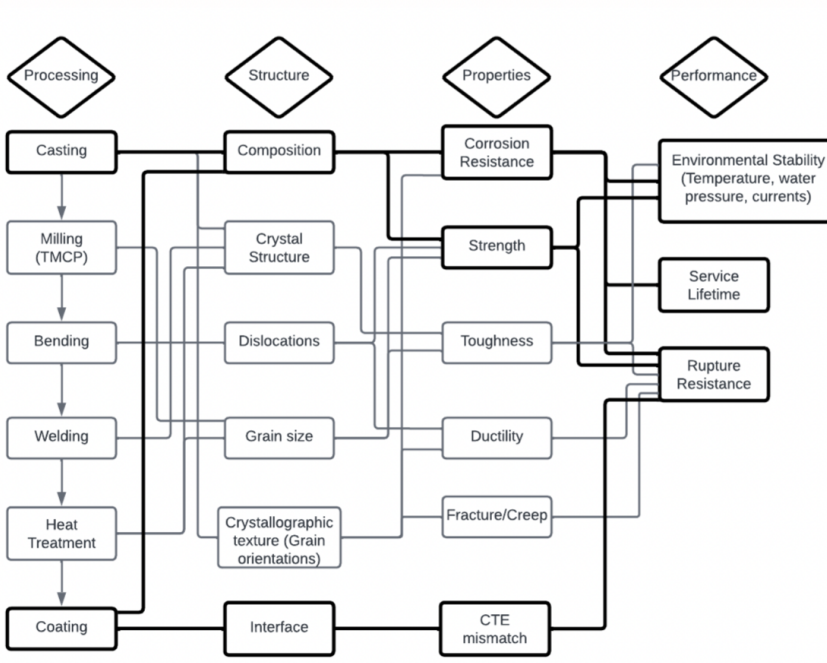

Figure 2: System Design Chart

Materials Selection

Since our project focuses on corrosion, it is very important to ensure that the material selected for the pipeline has excellent resistance to the corrosive substances it is exposed to (salt water and weak acids which can form from CO_2 [6]. We set these constraints in Granta. Also important is that the price be reasonable; since the stainless steel typically used in pipelines is no more than \$3.1/kg; we therefore set this as an upper limit on cost [7]. Since mismatch in coefficient of thermal expansion can lead to coating delamination, it is also important to minimize the CTE mismatch between the pipe material and coating. We chose epoxy as the coating material for our analysis. Because the material can be subjected to temperatures between 5 and 100 Celsius, we determined that the minimum operating temperature must be no more than 5 Celsius and the maximum operating temperature must be no less than 100 Celsius. Additionally, it is critical to avoid "fast fracture," since this would lead to oil or gas leaking into the sur-

rounding environment; the likelihood of this can be minimized by maximizing the fracture toughness, K_{1C} [8].

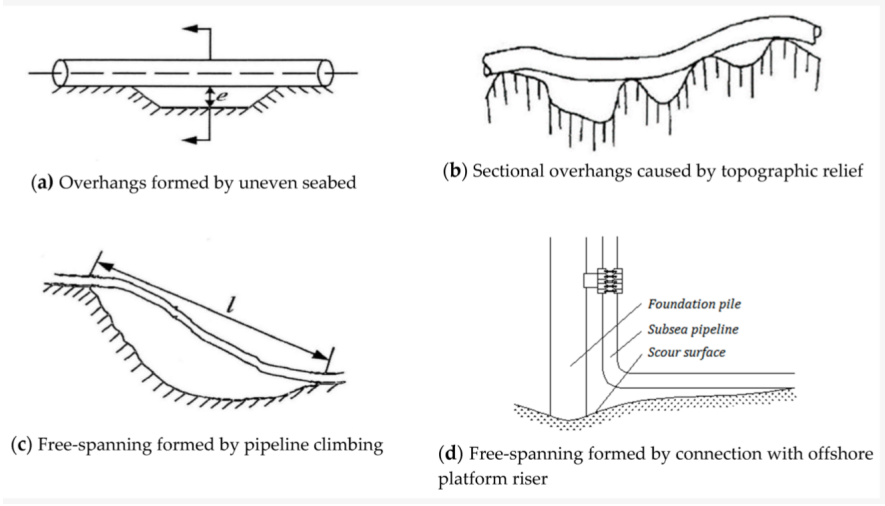

Figure 3: Pipeline conditions due to topography of seabed [9]

Due to unevenness in the seabed, some segments of the pipeline will be subjected to bending loads which can be modeled as simply supported beams subjected to distributed loads (see Figures 3 & 4).

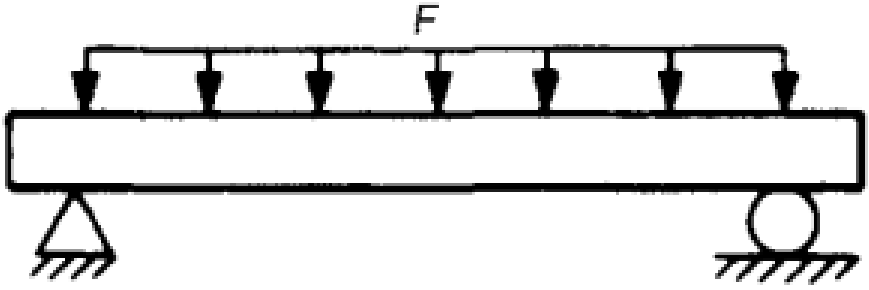

Figure 4: Bending [8]

The total force experienced at failure will by given by

$$F_{tot} = CH\sigma_y/L$$

,

where L is the length of the pipe, σ_y is the yield stress, and C and H are determined by the loading condition and cross section, respectively [8]. Ashby gives $H \approx 2\pi r^2 t$, where r is the radius of the pipe and t is the thickness, which is proportional to $V^{1/3}$ [8]. Since $\rho = \frac{m}{V}$, H is dependent on $\rho^{-1/3}$. Therefore, to minimize the applied force we must maximize

$$M_1 = \frac{\sigma_y}{\rho^{1/3}}$$

.

This is our performance index for bending.

The pressures the pipes are subjected to in deep water can lead to buckling, which is more likely if the material is less stiff. [10]. We can model the pipe in this scenario as a thin-walled tube which can withstand pressures up to p'_{crit}:

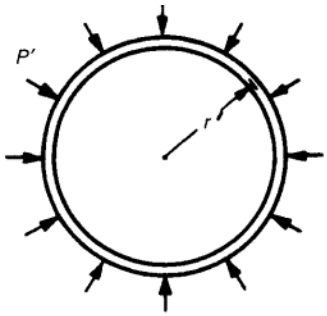

$$p'_{\text{CRIT}} = \frac{3EI}{(r')^3}$$

Figure 5: Thin-walled tube subjected to internal pressure [8]

In this case, $I \approx \pi r^3 t$ [8]. This means that I is propotional to $\frac{1}{\rho^{1/3}}$ such that our index for buckling is

$$M_2 = \frac{E}{\rho^{1/3}}.$$

We aimed to maximize these two indices by plotting selection lines for these two indices in GRANTA and applying our constraints. We then aimed to see which candidate materials had the highest fracture toughness and most similar thermal expansion coefficient to epoxy.

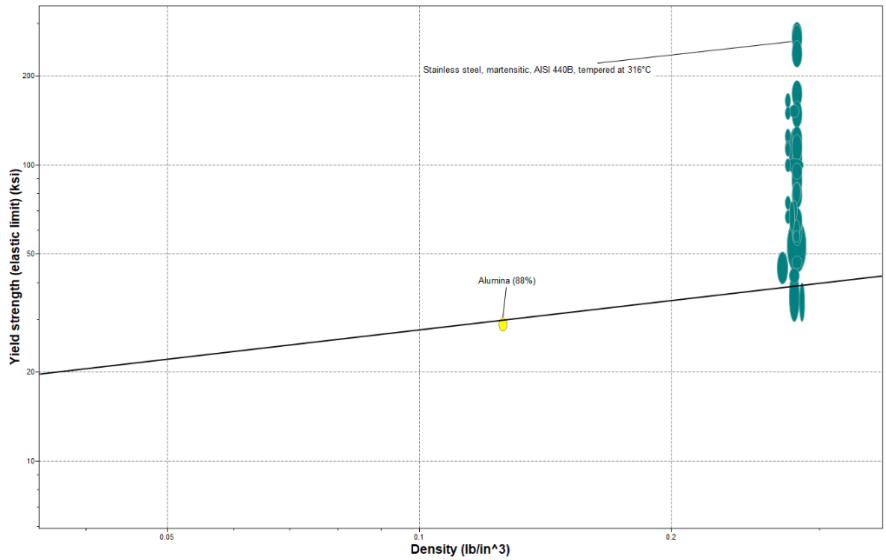

Figure 6: σ_y vs. ρ with selection line shown

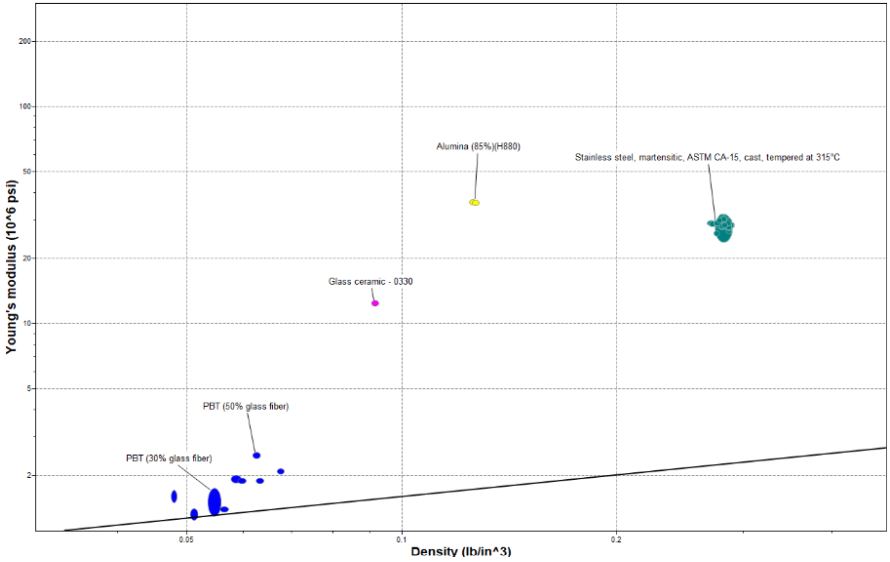

Figure 7: E vs. ρ with selection line shown

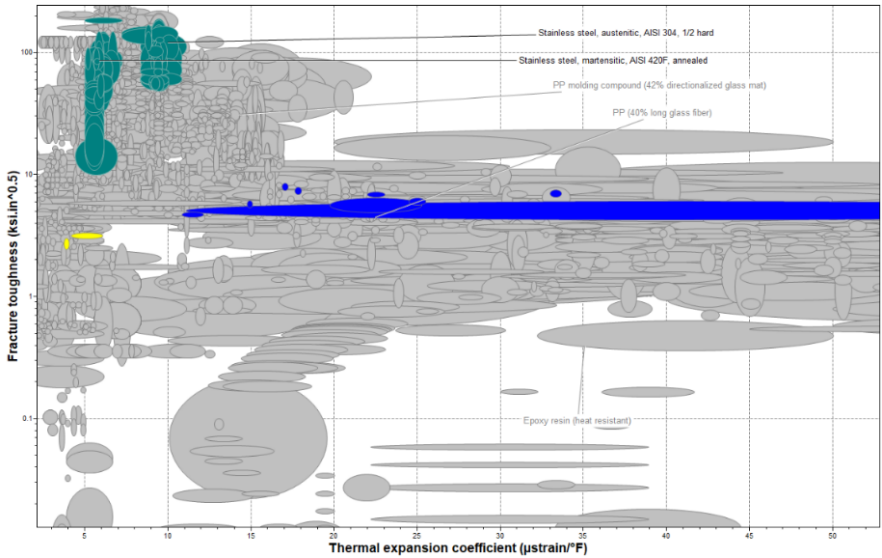

Figure 8: K_{IC} vs. CTE

In terms of strength, stainless steels-particularly, martensitic stainless steels-have the best performance (see Figure 5). Considering modulus, stainless steels are second best with alumina being a better option (see Figure 6). After stainless steels and alumina, there are several polymer-based composites that are significantly lighter but have much lower moduli and strengths (see Figures 5 & And 6).

When thermal expansion is considered, polymer-based composites are most similar to epoxy, followed by austenitic stainless steels (see Figure 7). However, stainless steels-particularly, austenitic stainless steels-have fracture toughnesses an order of magnitude higher (See Figure 7). Alumina's low fracture toughness makes it a less desirable material. Overall, the best candidate seems to be austenitic stainless steels. This is consistent with industry trends, where austenitic stainless steels like 316-grade stainless steel are commonly used [11].

Design Strategy

Having selected our material, our design strategy focuses on adding a coating of passivating metal to protect the underlying stainless steel (see Figure 9)

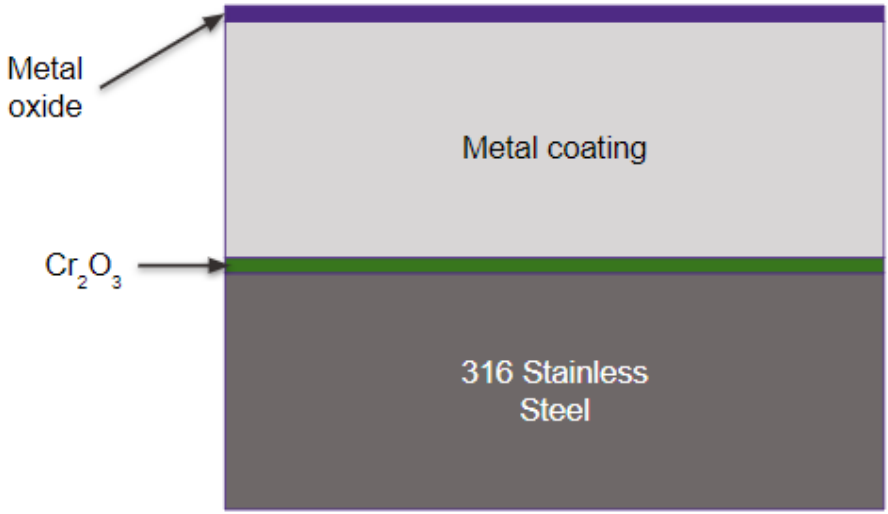

Figure 9: Diagram showing surface of pipe with metallic coating

Additional coatings such as epoxy can be applied on top of the metallic coating. Our goal is to maximize the ease with which oxidation can occur.

Coating & Process

To determine which metals would react with O_2 most readily, we turned to the activity series, which ranks metals according to their ease of oxidation [12]. We aimed to find elements which oxidized at least as readily as Cr and found that the candidates are: Li, Rb, K, Ba, Ca, Na, Mg, Al, Mn, & Zn [12].

From the potential coating materials in the previous section, we filtered out elements with negligible solubility in Fe between 5 and 100 Celsius because if they diffused into the steel they would form precipitates which would change the properties of the steel. To accomplish this, we reviewed phase diagrams in the existing literature to narrow the list of candidates.

We also ensured that the costs of our candidate materials and processes were feasible.

Diffusion Simulation

Having selected our optimal coating material we used diffusion profiles on ThermoCalc's Diffusion Controlled Transformation (DICTRA) to analyze a simplified version of our multi-component system to determine whether significant amounts of coating diffused into the pipe at 100 Celsius. This was important because even if the coating material did not precipitate in pure iron, there remained a risk of precipitates forming with alloying elements such as Cr [13]. For this reason, we aimed to ensure that very little diffusion would occur between the coating and steel over a service life of several decades. Our system consisted of our bulk material (stainless steel with added elements) and a layer of coating metal. This simulation did not account for the CrO_2 passivation layer which a real stainless steel would have (Thermo-Calc does not have much information on oxides); it therefore overestimated the diffusion depths, providing us with a diffusion depth in a worst-case scenario. We determined the depth to which the coating diffused into the steel (and vice versa), as well as the composition near the steel-coating interface.

Mechanical Model

In order to assess the materials selection of the pipe and coating, a simple computational model was developed COMSOL Multiphysics to compute the mechanical and thermal stresses acting on the pipe.

To simplify the model, the main forces acting upon the pipe consist of the external force resulting from hydrostatic and atmospheric pressures, as well as the internal pressure from the fluid flowing through the pipe. The pipe is modeled to be a cylindrical shell with the parameters shown in Table 1. Due to the considerable length of subsea pipelines, they typically consist of straight segments with minimal bends or curves. As a result, it is feasible to model these pipes as straight cylinders.

In addition, considering that there may be irregularities in the seabed surface, localized point pressures may be exerted on these pipelines. These point pressures can also be modeled and analyzed on COMSOL.

Table 1: Parameters to define the computational model of the pipe.

Parameter	Value
Outer diameter (m)	1.2 [15]
Wall thickness (mm)	40 [15]
Water depth (m)	600 [15]
External pressure (MPa)	6.15
Internal pressure (MPa)	5 [14]
Pipe material	316 steel
Coating material	10 microns pure-Al coating

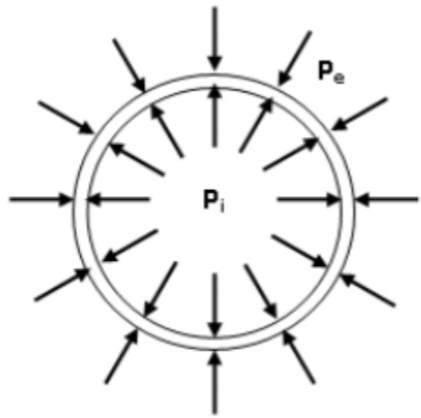

Figure 10: Internal and external load acting on the pipe surface [14]

Results

Coating & Process Selection

Our analysis of the candidate elements revealed that Al and Mn were the only candidates with significant solubilities in Fe at the operating temperatures of undersea pipelines [16–18].Because Al oxidizes more readily than Mn, being higher on the activity series, we chose to plate the steel pipes with Al to enhance the service lifetime of the pipe [12]. Al alloys have a CTE of 21.6-24.6 $\frac{\mu strain}{^\circ C}$, which is greater than that

of stainless steels (10.8-16.5 $\frac{\mu strain}{^{\circ}C}$) but less than that of epoxies (81-117 $\frac{\mu strain}{^{\circ}C}$) [7]. This makes Al a good candidate to be sandwiched between 316 stainless steel and epoxy as an additional layer of protection.

We used the Process Universe in Granta EduPack to determine the best surface treatment to protect the steel. Our goals were to minimize the temperature and coating thickness to minimize the chances of Al diffusing into the steel during the coating process and minimize the amount of excess Al used in the coating. Our selection constraints were that the process must provide protection from corrosion by water, gases, and organic substances, and be applicable to the curved surfaces of pipe segments. We applied these constraints using a Limit in Granta. Doing this left only two possible candidates: hot-dip coatings and boriding (see Figure 11).

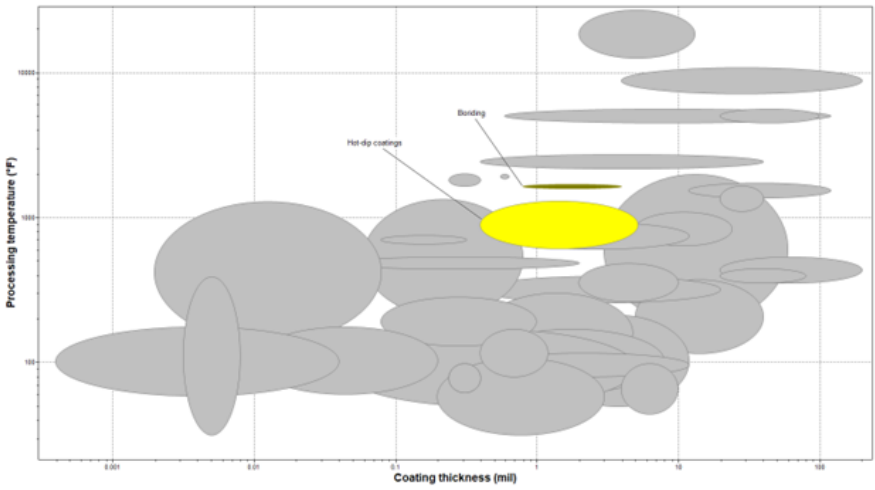

Figure 11: Ashby Chart for Coating Process Selection [**?**]

Since hot-dip coatings use lower temperatures, deposit thinner coatings, and can be used to apply Al (boriding consists of diffusing boron into the surface), this is the best process for our application [7]. Hot-dipping consists of placing a part, commonly stainless steel, in a molten metal with a low melting point such as Zn or Al, removing it, and blasting it with cold air to solidify the metal [7]. It is commonly done for stainless steels and can be used on parts as large as 30 x 2 x 4 meters (pipe segments are usually 12-24 meters long and typically have

diameters under 1 m) [7] [19] [20]. The coatings deposited by hot-dipping can be as thin as 10 microns, though they tend to be quite nonuniform and thickness is difficult to control [7]. Even for very large pieces, hot-dipping takes only a few minutes and produces coatings which are very resistant to mechanical damage and can protect steels for 30 years [7]. These factors make hot-dipping optimal for coating 316 stainless steel with Al.

The American Galvanizers Association ran a life-cycle analysis comparing the cost of hot-dip coatings with that of polymeric coatings for a bridge [21]. They found that the initial cost of hot-dip coatings was 2/3 that of epoxy-based coatings, while the overall life-cycle cost was 1/10 that of the epoxy coatings [21]. This illustrates that hot-dip coating would be a cost-effective means of either replacing epoxy-based coatings or providing an additional layer of protection to stainless steel pipes.

Diffusion Simulation

We ran a simplified DICTRA simulation using the TCFE9 Steel/FE-Alloys v9.3 Database and MOB2: Alloys Mobility v2.7 Database in Thermocalc. The phases selected included austenitic steel at a composition of Fe-0.15wt%C-12wt%Cr bulk and 100% aluminum layer. This simplified model was used as it simulated the layering of aluminum oxide- aluminum-bulk austenitic steel. We where primarily concerned about the diffusion of aluminum into the bulk austenitic steel along with the diffusion of the iron and chromium into the passivation layer=.The geometry was kept as planar and the model used a geometric 1.10 point type, with a width of 50 nanometers and 200 points. The left interface composition was fixed as 100 wt% Al and the right interphase was closed. We investigated the diffusion of the Al at an isothermal temperature of 100 degrees Celsius (the upper operating temperature from our preliminary investigations). We ran our simulation for 1e9 seconds, which is approximately 31.7 years, within the common operating lifetime of the pipelines. In our model, a 0.01wt% of Al was introduced into the steel because the software required all elements to be present in the bulk.

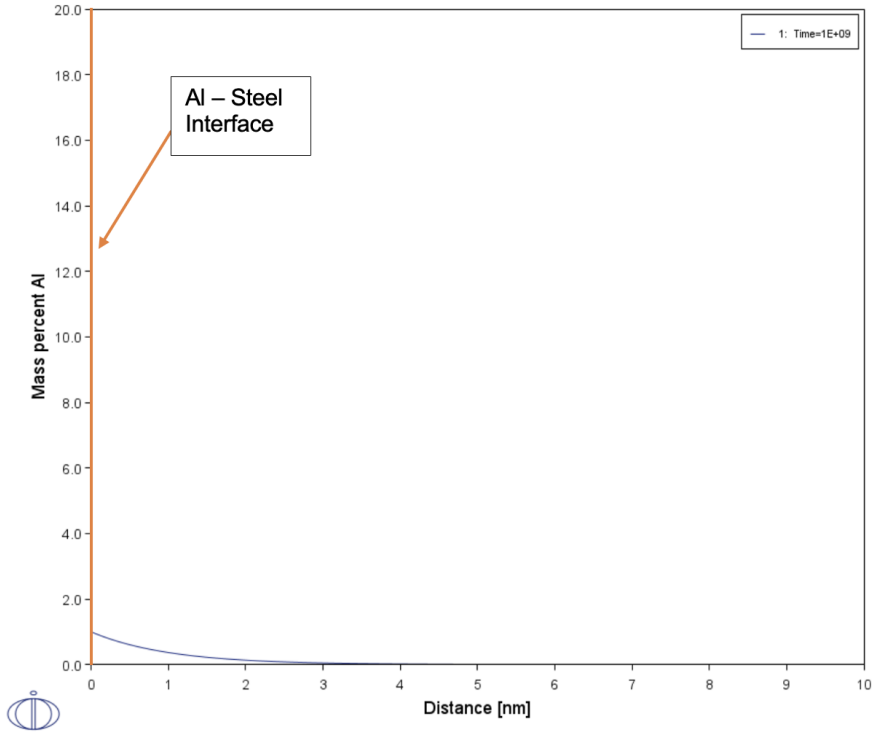

Figure 12: Al Diffusion into bulk material for 31.7 years at 100°C

Prior to our results, we hypothesized that diffusion of minority elements layers would not have played a significant role given the relatively low operating temperature of the diffusion profiles. Our results also indicated that the Al diffusion into bulk austenitic steel is negligible over the pipeline's operating conditions, with Al only penetrating less than 10 nm of the bulk material. The surface concentration of Al remains less than 2%, meaning that the likelihood of Al-Cr precipitates forming is very low. This is a promising discovery that supports the use of Al as an additional layer of protection for the pipe.

Given our concerns for the precipitation of Aluminum-Chromium-Iron phases, we also investigated the diffusion of Cr into the Al passivation layer to develop a more comprehensive view of the concentration profiles across the Al-steel interface [13]. We used a 10 nm Al phase layer and a right interface of our Fe-0.15wt%C-12wt%Cr and plotted the diffusion profiles are presented in the below figures.

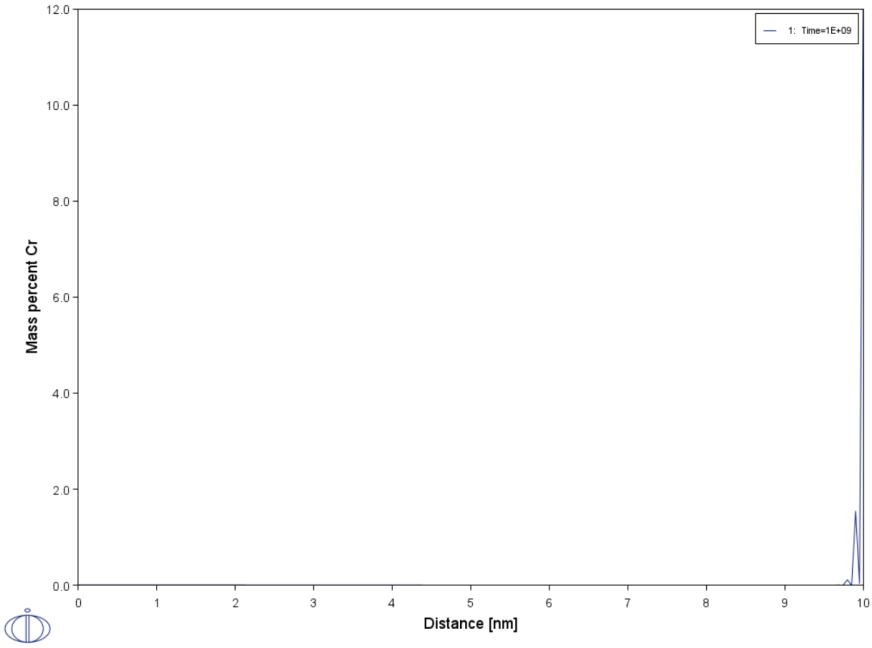

Figure 13: Cr Diffusion into Al layer for 31.7 years at 100°C

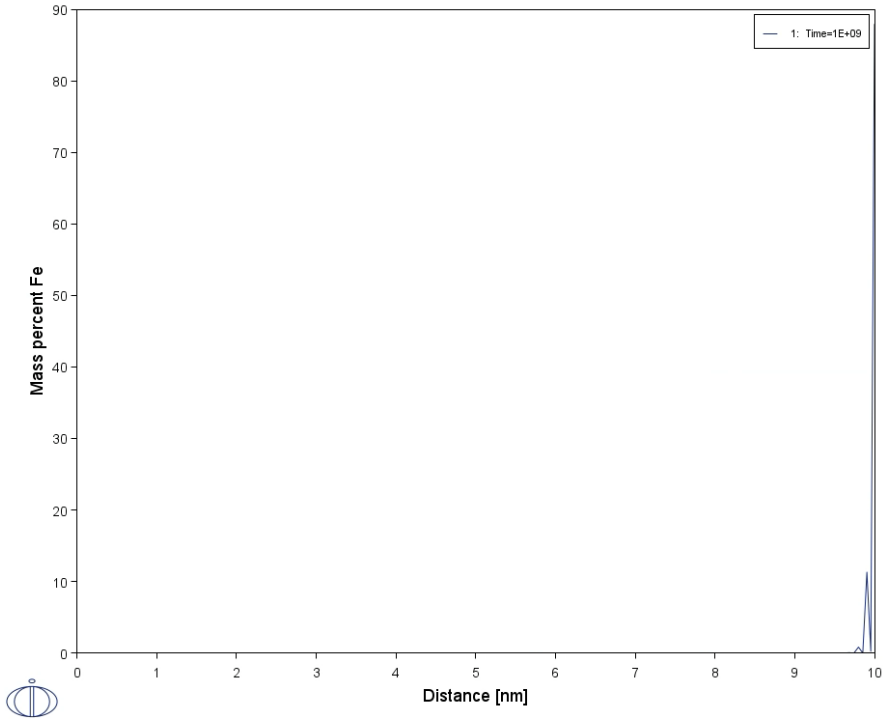

Figure 14: Fe Diffusion into Al layer for 31.7 years at 100°C

Again, from these results, we see that there appears to be very little diffusion of minority elements into the respective layers. These further illustrate the stability of Al coatings as a means of protecting the pipes over decades of service.

Mechanical Model

Figure 15 shows the initial temperatures of the inner and outer surfaces of the pipe of 100°C and 5°C respectively.

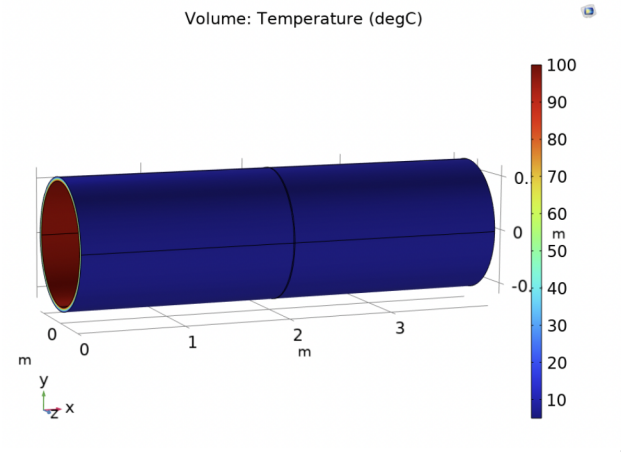

Figure 15: COMSOL Multiphysics model of a cylinder. Outer surface temperature is 100°C and inner surface temperature is 5°C.

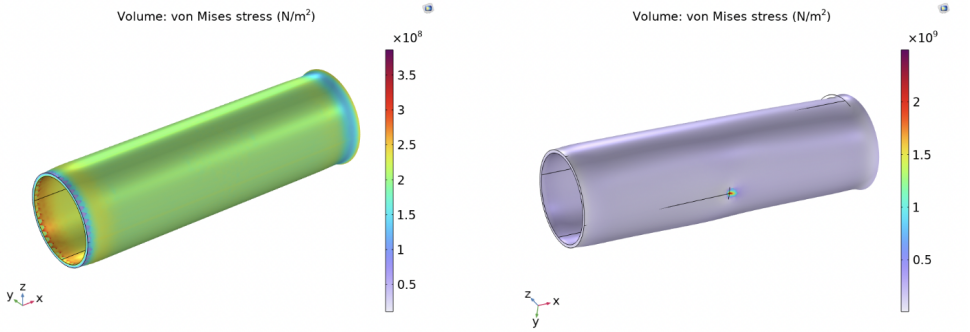

Figure 16: (Left) Stress in the pipe due to mechanical load and thermal expansion. Left boundary (in -x direction) is fixed. Maximum stress of 300 MPa on the inner surface of the fixed end. (Right) Adding fixed point on the bottom of the pipe to model force due to pipe bracket or other point force

Figure 16 shows that the maximum stress is acting on the fixed end, as expected, with a maximum value of around 400 MPa. When a point force is acting on the pipe, the maximum stress around the point can go up to 2.5 GPa - although the dimension and direction of the point load is unlikely in real conditions. However, it is important to

consider that unevenness of external loads can potentially cause crack and eventual failure over time. Nevertheless, considering that these models are simulated in steady-state conditions, the results show that the pipes would be able to withstand the expected loads for a long time.

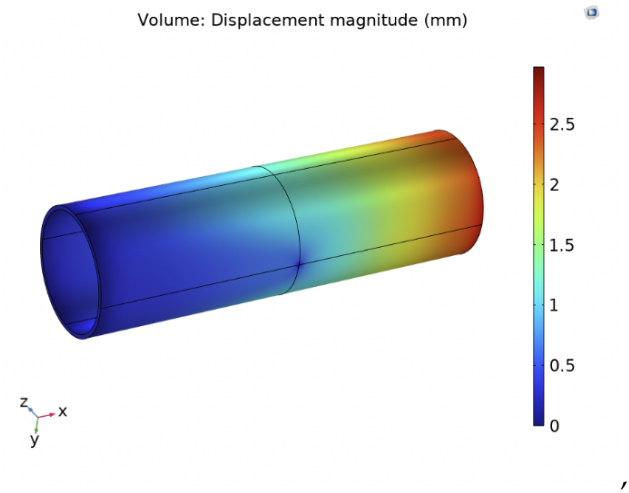

Figure 17: Resulting net displacement due to thermal stress expanding the pipe, and mechanical load compressing the pipe inwards

Finally, the results show that the pipe will experience a maximum displacement of around 3 mm, which is about 7.5 % of the wall thickness. If the pipe is to be encapsulated within a rigid protective layer such as concrete, it is crucial to consider its expansion. The dimensions of the protective layer should allow sufficient space for the pipe to expand without experiencing constraints or excessive stress.

Recommendations

Our investigation has revealed that coating 316 stainless steel pipes with Al would result in a passivation layer which could impart decades of additional protection to critical infrastructure without significantly affecting the composition or performance of the underlying steel. Hot-dip coating processes could be used to economically apply this coating to large pipe segments. This coating could be used instead of

or in addition to other protective measures such as epoxy coatings. FEM analysis shows that the stresses introduced by CTE mismatch between coating and substrate would not compromise the pipe's performance.

Future Work

If more time had been available, additional aspects of this design could be explored. Our analysis was entirely computational; experimental validation of the design would better illustrate its viability. We could acquire 316 SS coupons, dip them in molten Al, and blast them with cold air to solidify the coating using equipment such as furnaces and compressed air cans available in Cook Hall. Aging these coupons at elevated temperatures could simulate the decades-long lifetimes of the pipes on a much faster scale. We could use SEM and EDS to validate that interdiffusion between the Al coating and steel would be minimal over the pipe's lifetime. Additionally, we could expose one side of a coupon to $100°C$ and the other to $5°C$ and check the surface for cracking using optical microscopy; this would illustrate whether the coating was able to withstand the thermal stresses to which it was subjected. Dropping a coupon on gravel and then exposing it to salt water and gasoline at high temperatures could validate the ability of the coated material to resist corrosion after damage during transport or installation.

In addition, welding residual stress is a well-known factor that can contribute to pipe failure. To assess the resulting stress and expected lifetime of the pipes, it would have been beneficial to model the welding joints between pipes. However, due to limitations in the COMSOL software and limited expertise in structural analysis and welding methods, it was not feasible to perform such assessments within the available timeframe.

We could also have performed our own lifecycle analysis to evaluate the impact of our coatings on pipeline cost. The existing lifecycle analysis we found for hot-dip galvanization was for a bridge and used Zn instead of Al [21]. While this was sufficient to illustrate the merits of hot-dip coatings relative to polymeric ones, the quantitative effect of hot-dip Al coatings on pipeline cost will be different because

of the expenses associated with materials, manufacturing, transportation, maintenance, and operation. A comprehensive analysis of these factors would allow oil and gas companies to make confident and informed decisions regarding how best to protect their pipelines.

Contributions

- Conor: Pipe materials selection, coating materials & process selection
- Steven: Pipe materials selection, DICTRA simulations
- Nadiah: Precipitation research, FEM simulations
- All: report writing and editing

References

[1] J. Koto, J. A. Khair, A. Selamat, Ultra deep water pipeline design and assessment, Proceeding of Ocean, Mechanical, and Aerospace-Science Engineering- 2.

[2] Subsea pipeline engineering, oil and gas, uk.

[3] D.-S. Park, Y.-K. Seo, A study on heat loss from offshore pipelines depending on the thermal conductivity of backfills and burial depth (2018) 001–006.

[4] Api 1111, design, construction, operation, and maintenance of offshore.

[5] N. S. Corporation, Uoe pipe.

[6] I. Michael Baker Jr., R. R. P. Fessler, Pipeline corrosion-final report (2008) 22.

[7] Granta, Granta design studio.

[8] M. F. Ashby, Materials selection in mechanical design, 2nd edition (1999) 379, 383, 385, 417, 481.

[9] B. Zhang, G. Rui, T. Wang, Z. Wang, Causes and treatment measures of submarine pipeline free-spanning, J. Mar. Sci. Eng. 8(5) (2020) 329.

[10] R. W. Bonds, Critical buckling pressure for ductile iron pipe.

[11] G. Schiorky, A. Dam, A. Okeremi, C. Speed, Pitting and crevice corrosion of offshore stainless steel tubing.

[12] P. J. Grandinetti, Activity series.

[13] L. Wu, J. Qin, V. O. Kharchenko, D. O. Kharchenko, O. B. Lysenko, Phase-field modeling of microstructural evolution of fe-cr-al systems at thermal treatment.

[14] A. A. Jaoude, H. Noura, E.-T. Khaled, S. Kadry, M. Ouladsine, Lifetime analytic prognostic for petrochemical pipes subject to fatigue., IFAC Proceedings Volumes 45 (20) (2012) 707–713.

[15] U. M. Company, Large diameter pipes (2012).
URL https://omksteel.com/upload/iblock/3f9/OMK%20large%20diameter%20pipes%20catalogue.pdf

[16] Al-fe phase diagram (2007).
URL http://www.gotrawama.eu/NIMSMIRROR/www.nims.go.jp/cmsc/pst/database/al-elem/alfe/alfe.html

[17] W. Tofaute, K. Linden, Fe-mn binary phase diagram 0-28 at.% mn (2022).
URL https://materials.springer.com/isp/phase-diagram/docs/c_0104121

[18] Springer materials.
URL https://materials.springer.com/

[19] U. D. of Transportation, Phases of pipeline construction: An overview.

[20] M. van Driel, A. Mayants, A. Serebryakov, A. Sergienko, Designing large-diameter pipelines for deepwater installation.

[21] A. G. Association, Hot dip galvanized steel costs less, lasts longer.